Proceedings of the IASS Annual Symposium 2019 – Structural Membranes 2019
Form and Force
7 – 10 October 2019, Barcelona, Spain
C. Lázaro, K.-U. Bletzinger, E. Oñate (eds.)

Modern timber design approaches for traditional Japanese architecture: analytical, experimental, and numerical approaches for the *Nuki* joint

Demi FANG*[a], Julieta MORADEI[b], Jan BRÜTTING[c], Aliz FISCHER[b], Daniel K. LANDEZ[a], Benshun SHAO[b], Nick SHERROW-GROVES[b], Corentin FIVET[c], Caitlin MUELLER[a]

[a] Massachusetts Institute of Technology (MIT), Cambridge, MA, USA
*Corresponding author: dfang@mit.edu
[b] Arup, San Francisco, CA, USA
[c] Swiss Federal Institute of Technology (EPFL), Fribourg, Switzerland

Abstract

This work fully investigates a specific timber joinery connection via experimental, analytical, and numerical methods. The selected joint is the *Nuki* joint: a mortised column with through-beam tenon. The experimental approach takes advantage of digital fabrication to reduce variations introduced by hand fabrication while the analytical approach builds on state-of-the-art embedment stress models. Material tests are used to calibrate the non-linear finite element model and analysis of the connection. Furthermore, the difference in behavior between prototypes of various beam thicknesses is examined across analysis approaches. This work not only sets out a workflow for digital fabrication, physical testing, and structural analysis for more complex joinery geometries, but also discusses the challenges and relevance of its application towards a reference library of joinery connections for modern timber construction.

Keywords: timber, joinery, connections, Nuki joint, physical testing, finite element analysis, rotational stiffness

1. Introduction

Timber is one of the oldest known building materials in the world. In contrast to Western analogs, Asian timber construction is characterized by its high degree of specialization in joinery and by connections with interlocking geometries. The use of joinery connections largely faded with the introduction of metal fasteners that continue to dominate post-industrialization timber connections.

Timber structures have seen a revival in recent decades due to growing awareness of timber's reduced environmental footprint compared to typical building materials such as steel or concrete. Buildings are responsible for a third of global carbon emissions, and substituting wood for other materials could prevent 14-31% of those emissions [1]. Current mass timber construction uses steel connections (e.g. nail plates) which often results in a one-life span design of structures. The use of interlocking timber joinery can allow for more sustainable, non-destructive disassembly of timber structures, as demonstrated by historic precedents such as the *Ise* Shrines (Japan, 4 BC) [2].

The budding capabilities of today's digital fabrication technology offer an opportunity to revitalize the use of interlocking joinery in modern timber construction. Examples featuring 21st-century joinery connections include the Yusuhara Bridge Museum (Japan, 2010) by Kengo Kuma and Associates, the Tamedia Office Building (Switzerland, 2013) by Shigeru Ban Architects, and the Writers Theatre (USA, 2016) by Studio Gang Architects.

While there are benefits to reintroducing joinery connections into modern construction from the perspectives of sustainability, constructability, and fabrication capabilities, the main obstacle is to characterize and codify the mechanics of these connections. This paper is part of an ongoing investigation into a workflow aimed to build up centralized knowledge on joint behavior. In this paper the *Nuki* joint (Figure 1) is selected as an example to demonstrate the workflow. The simple geometry of the *Nuki* – a beam piercing through a mortised column – enables a clearer understanding of its mechanics, facilitating the calibration between analysis and experimental testing. This paper focuses on predicting the rotational stiffness and behavior of the joint. The key steps of the workflow are 1) the experimental testing of digitally fabricated specimens, 2) the analysis of the interlocking joint's behavior using principles of structural mechanics, and 3) the numerical simulation employing non-linear finite element analysis (FEA). The future aim of these calibrations is to enable the characterization of joints with more complex geometries and variations.

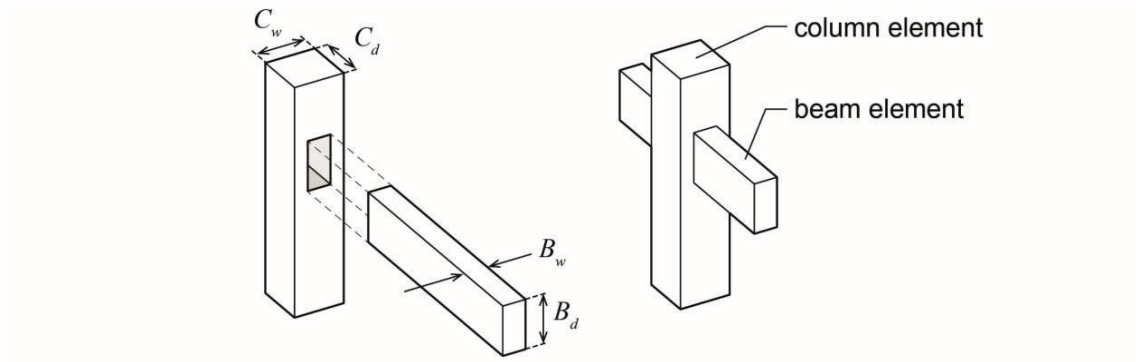

Figure 1. Nuki joint, a simple joinery connection studied in this work.

1.1 Literature review

Fascination with joinery connections from a historical and cultural point of view is evident from a number of books and studies cataloguing their origins, evolutions, and geometries [3], [4]. The analyses of timber joint mechanics range across analytical, numerical, and experimental methods. Some focus on validation between experimental and numerical methods [5], [6], while others use a variety of analytical models that are compared against physical tests [7]–[10]. A key behavior in the analysis of joinery connections is embedment [11], which refers to the compression of one joint element (or part) into another, a behavior that arises from the reduced stiffness of wood perpendicular to the grain. Building upon embedment theory, Kitamori et al. [12] showed that additional embedment length outside the direct contact region can significantly contribute to rotational stiffness. Komatsu et al. [12] considered an elastoplastic material behavior where only a reduced material stiffness is taken into account when the yield-point is reached, enabling an analytical description of the typical bi-linear moment-rotation behavior of semi-rigid joinery connections. Recent works have applied his theory to different joinery connections [13], [14]. As for the *Nuki* joint in particular, Chang et al. [15] compared analytical and experimental models but do not discuss plastic effects of the joint behavior. Guan et al. [6] compared experimental and numerical models for *Nuki* joints with wedges.

In summary, the state of the art for analyzing interlocking joinery through experimental testing, mechanical analysis, and numerical simulation have yet to be synthesized and calibrated. This work particularly builds on own previous work by Fang and Mueller [7], Moradei et al. [16], and Fang et al. [17]. This work presents new results on digitally fabricated specimens made of glue-laminated timber as well as numerical results to compare with the analytical and experimental approaches.

2. Methodology

The *Nuki* joint was here parameterized by beam depth B_d, beam width B_w, column width C_w, column depth C_d, which are notated in Figure 1. For experimental testing, joint specimens were manufactured with dimensions $B_d = C_w = C_d = 8.25$ cm. Two different beam widths B_w, 2.54 cm and 3.81 cm were studied. A visual overview of the experimental and numerical testing setup is shown in Figure 2.

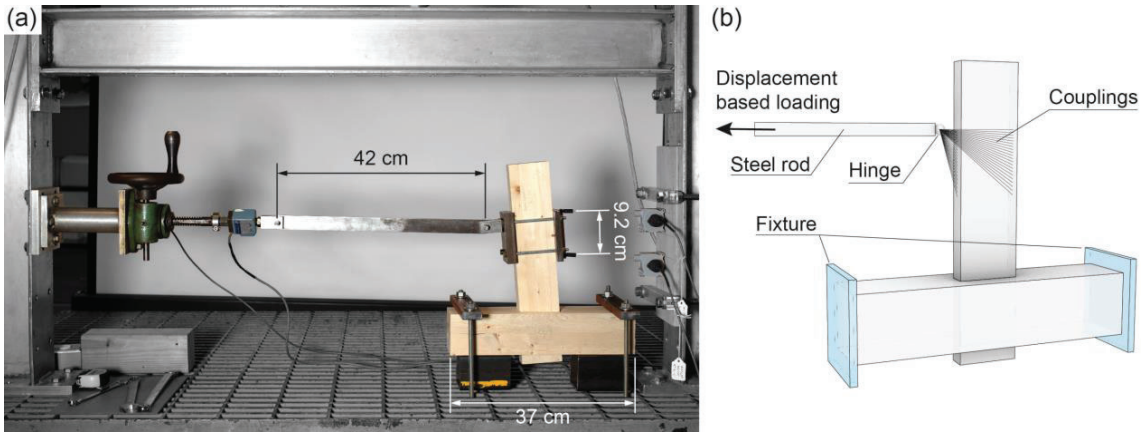

Figure 2. Setup, support and loading conditions of the (a) experimental testing and (b) numerical simulation.

2.1 Material properties

Glue-laminated timber elements were used for the experimental prototypes. Material testing was conducted first to determine the material properties and to apply them in the analytical and numerical models. Most relevant mechanical properties are summarized in Table 1.

Table 1. Mechanical properties determined for the material used in wood specimens.

$E_{c,0}$ Mean (standard dev.) [MPa]	$E_{c,90}$ Mean (standard dev.) [MPa]	$\varepsilon_{c,y,90}$ Mean (standard dev.) [m/m]	PR_{90} [%]
13,500 (1340)	385 (89)	0.025 (0.001)	11.8%

$E_{c,0}$ compressive stiffness (modulus of elasticity) parallel to grain
$E_{c,90}$ compressive stiffness (modulus of elasticity) perpendicular to grain
$\varepsilon_{c,y,90}$ yield compressive strain perpendicular to grain
PR_{90} reduced stiffness of $E_{c,90}$ after yielding

2.2 Experimental setup

Six glulam specimens for each joint geometry were digitally fabricated with a robotic CNC router. The opening in the columns has rounded corners equal to the size of router ball end, i.e. 9.5 mm. In the test setup, which is shown in Figure 2(a), the column element of the joint was fixed to the table, while the beam element was attached to a hand-screw-actuated load cell of 4400 N capacity. The beam-column connection was not press-fit, and varied in tightness. The total gap between the beam and column was in the 0-2 mm range. A linear displacement was applied at the beam end using the load cell, and the resulting rotation at the joint was measured by two string potentiometers.

2.3 Analytical model

The analytical model employed to prescribe the moment-rotation behavior of the joint is based on embedment theory and uses an elastic-plastic material model. In the model, the bending moment M is

expressed in terms of the rotation angle θ using trigonometric functions and structural mechanics. For details on the analytical model, the reader is referred to Fang et al. [17].

2.4 Numerical model

To numerically model the joint behavior, explicit finite element analysis was employed using the LS-Dyna v10.0 software package. Figure 2(b) illustrates the numerical simulation setup, designed to capture key aspects of the physical testing setup. The top and the bottom of the column are restrained from displacement and rotation. The surfaces where the loading clamp is installed are rigidly connected through their nodes. Those nodes are then coupled to the loading steel rod with a hinge. The loading is applied to the rod via a prescribed displacement that allows capture of the failure mechanism.

Beam and column are discretized with 45,000 fully integrated solid elements in total. A transversely anisotropic material model (LS-Dyna MAT 143) is employed for both components in the FEA analysis [18], [19]. This model allows to capture physically nonlinear effects (e.g. plasticity and damage) as well as the anisotropy between grain parallel and grain perpendicular behavior of the wood.

3. Results

The moment-rotation behavior obtained from all three models are summarized in Figure 3. The following subsections give detailed descriptions of each method's results.

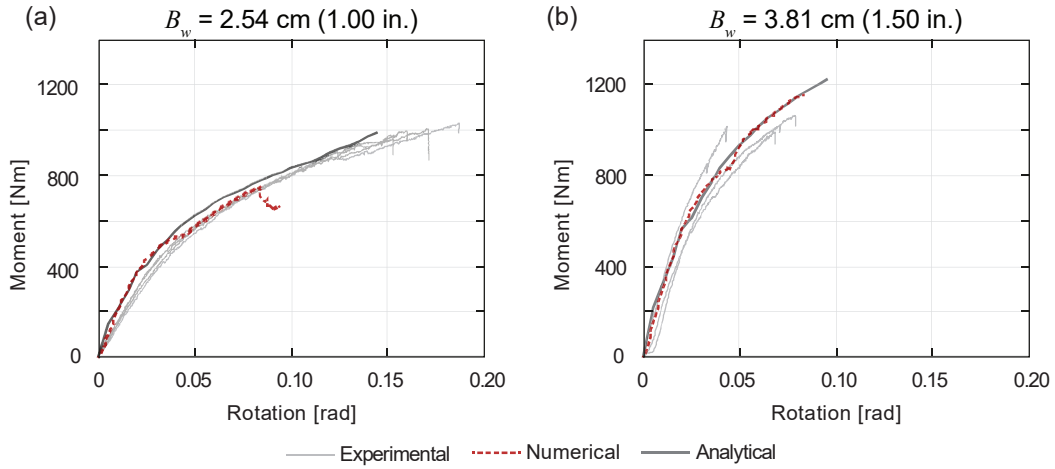

Figure 3. Summary of results from experimental, analytical, and numerical approaches. (a) Moment-rotation behavior for specimens of B_w = 2.54 cm; (b) moment-rotation behavior for specimens of B_w = 3.81 cm.

3.1 Experimental Results

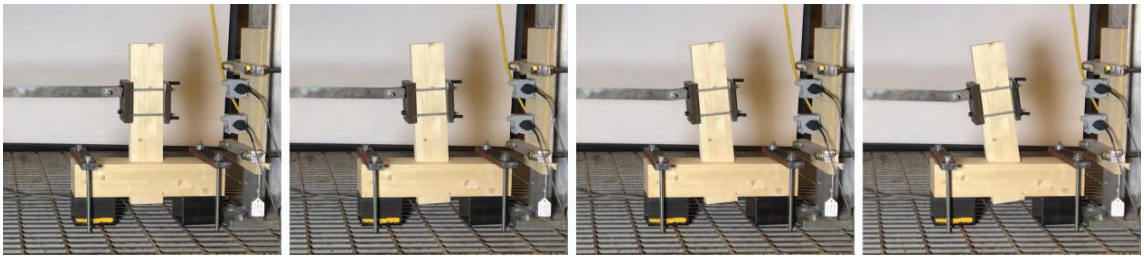

Figure 4. Rotational stiffness testing of prototypes. Progressive video frames from an example specimen.

Figure 4 shows a sequence of images taken during the experimental testing of one joint specimen. From the measured test data (Figure 3, grey) it is apparent that in general *Nuki* joints show a two-phase moment-rotation behavior: a first initial (linear elastic) stiffness and a second stiffness post-yielding. The change between the two phases happens gradually. Tests ended when the load cell reached its capacity. For nearly all specimens of B_w = 3.81 cm, this limitation prevented the estimate of secondary stiffness.

Variability in testing results is partially due to wood being a heterogeneous material. It can be further influenced by changes in temperature and humidity between fabrication and testing of the prototypes, as that affects the tightness of the fit between the beam and the column. Results could be more consistent with a much larger number of specimens.

3.2 Analytical results

The analytical model employs an elastic-plastic material behavior which is appropriate for describing the two-phase behavior demonstrated by the physical prototype. After calibration of the analytical model to the experimental test for both beam widths, one unique decay coefficient α was selected as $4.5/B_d$. This parameter relates to shape of the embedment outside the direct contact between beam and column. For α and all other parameters the reader is referred to Fang et al. [17]. The analytical model does not include failure prediction; the calculations were manually ended at 100 and 150 mrad for B_w = 2.54 cm and B_w = 3.81 cm, respectively. In general, after calibration the modeled rotation behavior matches the experimental data (Figure 3).

3.3 Numerical results

The main parameters of the material model, such as Young's moduli and strengths, were calibrated based on the physical material testing (see values in section 2.1). Other values, such as ν = 0.39 Poisson ratio, were estimated from literature [20]. Contact between beam and column is defined by numerical parameters representing the contact stiffness, the friction between surfaces, and the initial gap size. In the model, the gap size between the beam and the column was set up based on observation of the fabrication, with 0.5 mm gap each side of the beam. At the top and bottom the gap was smaller, 0.025 mm, to ensure numerical stability. The analysis assumed no initial stress from joining the two pieces.

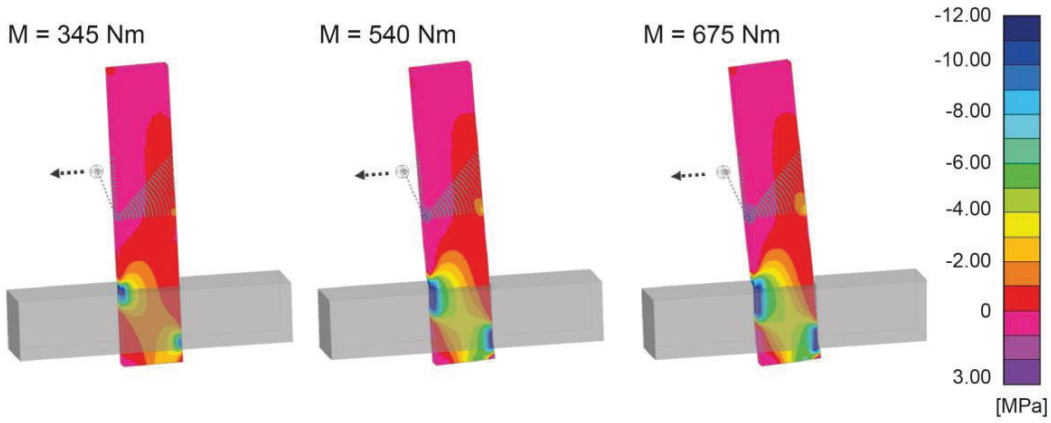

Figure 5. Stress in the beam perpendicular to grain (MPa) throughout the numerical simulation for the B_w = 2.54 cm specimen.

Selected images of the progression of the numerical simulation are shown in Figure 5. The contour plot shows the stresses perpendicular to the grain of the beam. The simulation was stopped when the analysis showed numerical instabilities as the damage at the contact became excessive. The stress distribution is in a good agreement with the assumption of the analytical model, and with the observations of the local

behavior at the physical testing. A close-up of the connection behavior for all three methodologies is shown in Figure 6.

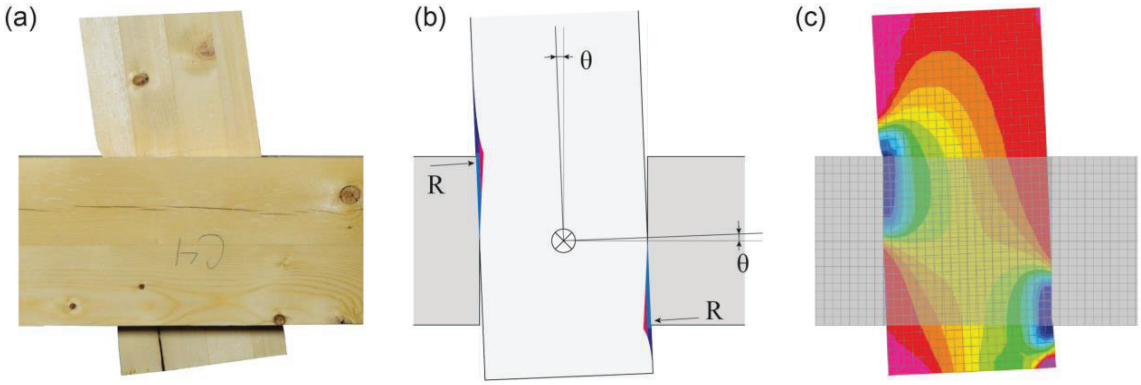

Figure 6. Close-up of the joint for (a) experimental testing, (b) analytical model, and (c) numerical simulation.

3.4 Comparison of stiffness values across models

In this section, based on the two-phase moment-rotation behavior, absolute and relative stiffness values are compared across all three models. 'Stiffness 1' refers to the initial stiffness, and 'Stiffness 2' refers to the post-yielding stiffness. Table 2 compares the absolute stiffness values. Table 3 compares the relative increase in stiffness with respect to the two tested beam widths. Note that Stiffness 2 values for the experimental testing of specimen with B_w = 3.81 cm are not recorded because experimental testing had to be halted before a post-yielding stiffness could be observed.

Table 2. Comparison of absolute stiffnesses across models.

	B_w = 2.54 cm		B_w = 3.81 cm	
	Stiffness 1 [kN-m/rad]	Stiffness 2 [kN-m/rad]	Stiffness 1 [kN-m/rad]	Stiffness 2 [kN-m/rad]
Experimental mean	16.0	5.46	25.1	--
Analytical model	18.7	4.29	28.0	6.44
Numerical model	18.9	5.10	28.1	6.74
% difference between analytical and experimental*	+17%	-21%	+10%	--
% difference between numerical and experimental*	+18%	-7%	+11%	--

* signed percent error assuming experimental mean as the 'expected value'

The results in Table 2 demonstrate that the analytical and numerical models overestimate the initial stiffnesses (Stiffness 1) by about 18% and 11% for the two different beam widths respectively.

Table 3. Comparing effects of beam width variation across models.

	% increase in stiffness between B_w = 2.54 cm and B_w = 3.81 cm	
	Stiffness 1	Stiffness 2
Experimental	57%	--
Numerical	49%	32%
Analytical	50%	50%

The results in Table 3 demonstrate that in the experiments there is a slightly larger relative increase in initial stiffness from increasing beam width than numerically and analytically predicted.

4. Conclusion and future work

The rotational stiffness of *Nuki* joints was tested with digitally fabricated specimens made of glue-laminated timber. The rotational behavior was modeled both analytically and numerically, and these models were calibrated with the experimental results through material testing. While neither model captures wood behavior at a micro level, calibrating key parameters allowed analytical and numerical models to capture the overall behavior of the joints. For behavior at failure, the models were more limited: the analytical model does not capture failure by definition, while the numerical model resulted in numerical instabilities as the local failure at the contact surface became excessive. However, the accuracy of failure prediction is not crucial because for design recommendations, the region of initial stiffness will be of primary interest.

While digital fabrication allowed quick and precision woodwork, the variability of the wood due to change in humidity or temperature over time did not allow the connection fit to be precise. In practice, majority of the typical connections are press-fit, eliminating this issue. For non-press-fit connections, more care needs to be taken to the consistency of the fabrication environment for precise fit. Design values also need to be defined considering this variability. In the future, further experimental testing could increase the number of specimens and improve the consistency of results against both models to verify that all parameters result in model predictions close to expected behavior.

This paper demonstrated analytical and numerical models effectively predicting rotational stiffness behavior and absolute values within 20% of experimental results after material calibration. With the now calibrated model parameters it is possible to analyze other joint types and geometries. MAT 143 material also proved to be suitable to numerically simulate other joint geometries, allowing the numerical design of more complex connections where analytical models are not available. Further, the obtained semi rigid moment-rotation behavior could be integrated into a global FEA model via rotational springs.

Overall, the potential for both models to be used for other joinery geometries was demonstrated. This workflow can be applied to further joinery connections in an effort to build up a centralized knowledge base of joinery connections, empowering designers to apply these historically-inspired, sustainable connections more widely in timber construction.

Acknowledgements

The authors would like to acknowledge Nordic Structures and Bensonwood for providing the prototype material, Autodesk BUILD Space for the fabrication facilities, Arup's internal research grant for funding JM, AF, BS, and NSG, and Stephen Rudolph at MIT CEE for assisting the physical tests.

Author Contributions

DF, JB, and CM developed the analytical model. DKL and DF carried out digital fabrication and physical testing. AF, BS, and JB built and analyzed the numerical model. DF and JM provided overall coordination and management. NSG, CF, and CM supervised.

References

[1] C. D. Oliver, N. T. Nassar, B. R. Lippke, and J. B. McCarter, "Carbon, Fossil Fuel, and Biodiversity Mitigation With Wood and Forests," *J. Sustain. For.*, vol. 33, no. 3, pp. 248–275, Apr. 2014.

[2] C. Henrichsen and R. Bauer, *Japan Culture of Wood: Buildings, Objects,Techniques*, 1 edition. Boston: Birkhauser, 2004.

[3] T. Sumiyoshi and G. Matsui, *Wood Joints in Classical Japanese Architecture*. Kajima Institute Publishing Co. Ltd, 1991.
[4] K. Zwerger, *Wood and Wood Joints*, 3rd ed. edition. Basel ; Boston: Birkhäuser, 2015.
[5] E. M. Lang and T. Fodor, "Finite Element Analysis of Cross-halved Joints for Structural Composites," *Wood Fiber Sci.*, vol. 34, no. 2, pp. 251–265, Jun. 2007.
[6] Z. W. Guan, A. Kitamori, and K. Komatsu, "Experimental study and finite element modelling of Japanese 'Nuki' joints — Part two: Racking resistance subjected to different wedge configurations," *Eng. Struct.*, vol. 30, no. 7, pp. 2041–2049, Jul. 2008.
[7] D. Fang and C. Mueller, "Joinery connections in timber frames: analytical and experimental explorations of structural behavior," in *Proceedings of the International Association for Shell and Spatial Structures (IASS) Symposium*, Cambridge, MA, USA, 2018.
[8] R. J. Schmidt and R. B. Mackay, "Timber frame tension joinery," MSc thesis, University of Wyoming, Laramie, WY, 1997.
[9] J. Shanks and P. Walker, "Strength and Stiffness of All-Timber Pegged Connections," *J. Mater. Civ. Eng.*, vol. 21, no. 1, pp. 10–18, Jan. 2009.
[10] M. G. Shope, "Strength characterization of wood to wood connections using stress field analysis," Thesis, Massachusetts Institute of Technology, 2016.
[11] M. Inayama, "Wooden embedment theory and its application," PhD, University of Tokyo, Tokyo, Japan, 1991.
[12] A. Kitamori, T. Kataoka, and K. Komatsu, "Effect of Additional Length on Partial Compression Perpendicular to the Grain of Wood," *J. Struct. Constr. Eng.*, vol. 74, p. 642, 2009.
[13] K. Ogawa, Y. Sasaki, and M. Yamasaki, "Theoretical modeling and experimental study of Japanese 'Watari-ago' joints," *J. Wood Sci.*, vol. 61, no. 5, pp. 481–491, Oct. 2015.
[14] S.-Y. Yeo, K. Komatsu, M.-F. Hsu, Y.-L. Chung, and W.-S. Chang, "Structural behavior of traditional Dieh-Dou timber main frame," *Int. J. Archit. Herit.*, pp. 1–23, Mar. 2018.
[15] W.-S. Chang, M.-F. Hsu, and K. Komatsu, "Rotational performance of traditional Nuki joints with gap I: theory and verification," *J. Wood Sci.*, vol. 52, no. 1, pp. 58–62, Feb. 2006.
[16] J. Moradei *et al.*, "Structural Characterization of Traditional Moment-Resisting Timber Joinery," in *Proceedings of the International Association for Shell and Spatial Structures (IASS) Symposium*, Cambridge, MA, USA, 2018.
[17] D. L. Fang, J. Brütting, J. Moradei, C. Fivet, and C. T. Mueller, "Rotational stiffness in timber joinery connections: analytical and experimental characterizations of the Nuki joint," presented at the 4th International Conference on Structures and Architecture, Lisbon, Portugal, 2019.
[18] Livermore Software Technology Corporation, *LS-DYNA Keyword User's Manual: Material Models*, vol. 2. Livermore, California: Livermore Software Technology Corporation, 2018.
[19] Federal Highway Administration, "Manual for LS-DYNA Wood Material Model 143," US Department of Transportation, McLean, Virginia, Manual FHWA-HRT-04-097, Aug. 2007.
[20] Forest Products Laboratory, "Wood Handbook: Wood as an Engineering material," U.S. Department of Agriculture, Forest Service, Forest Products Laboratory, Madison, WI, General Technical Report FPL-GTR-190, Apr. 2010.